Characterization of a Reference Test Setup for the Development of HPEM Standards

Thorsten R. Pusch, Michael Suhrke, *Senior Member, IEEE*, and Benjamin Jörres

***Abstract*—Given that intentional interference with electronic devices is not bound by legal parameter limitations, formulating standard procedures to adequately probe device immunity poses a challenge. In order to foster such developments, we further characterize a compact reference test setup conceived earlier by new parameter studies. To acquire immunity profiles in a TEM waveguide, we used narrowband pulses similar to radar. Since the error threshold field values can depend on the angle of incidence of the incoming waves, we did an extended study over different orientations of our setup, only resulting in moderate variations. Together with measurements in the previously unexplored range between 4 and 8 GHz evidencing many error occurrences, we could show the versatility of our battery-operated reference test setup based on a single board computer of the Raspberry Pi line.**

***Index Terms*—High power electromagnetics, intentional electromagnetic interference, standard development, reference test setup.**

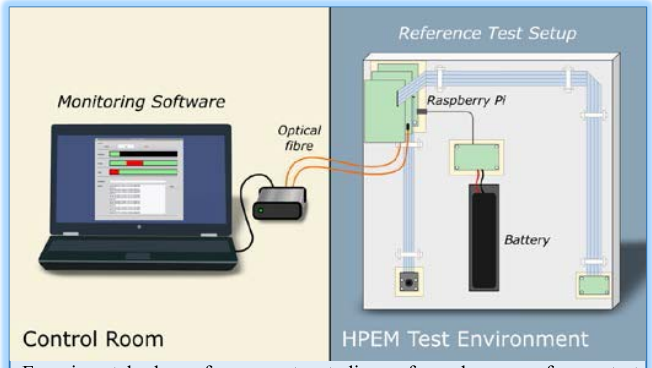

Experimental scheme for parameter studies performed on our reference test setup intended for comparison of test environments. (Visual Summary)

I. Introduction

INTENTIONAL attempts at interfering with regular operation of electronic devices by applying electromagnetic fields well beyond exposure bounds of product qualification EMC typically run under the umbrella term of IEMI (Intentional Electromagnetic Interference) or HPEM (High Power Electromagnetics). Given their unregulated nature, any attempt at deriving standard prescriptions for evaluating device immunity under these harsh conditions is facing a challenge. In contrast with emission and immission limits well regulated by law and thus facilitating regular EMC measurements, wide ranges of signal parameters spanning several magnitudes of dynamic range will have to be considered. Still, comprehensiveness will have to be balanced against resources available for qualification. The growing importance of new test environments in the high-power regime, such as the reverberation chamber (RC), raises additional questions regarding the transfer and the comparison of results across different facilities.

When addressing these questions in the ongoing development process of civil high-power EMC standards like the IEC 61000-5-9 [1] or IEC 61000-4-36 [2] as well as their military counterparts like NATO AECTP 500 [3], tightly controlled experimental conditions facilitate the assessments of the methods and the procedures. In that vein, together with colleagues from WIS Munster (Germany) and FOI (Sweden), we proposed the concept of a compact, reliable reference test setup as a means to minimize the influence of the device under test (DUT) itself to the measurements, possibly allowing to more clearly probe the intricacies on the test environment side [4].

While a few attempts at suggesting a reference setup have been witnessed in the past, mostly driven by normative validation prescriptions and e.g., foreseeing an unpowered [5] or galvanically connected DUT [6], our battery-driven proposition minimizes external connections to serial communication via optical fibre, allowing for constant monitoring under exposure while narrowing down on possible coupling paths. After having shown the general suitability of our setup for the intended purpose [4], including an investigation regarding the moderate influence of series variations, we do propose here an additional characterization study. While part of the results had already been discussed in [7], we have extended our

Take-Home Messages:

1. We combined an affordable single board computer with periphery to conceive a reliable reference test setup for high power electromagnetic immunity testing.
2. The setup consistently shows reproducible errors over a wide range of frequencies and test parameters.
3. This allows to probe differences between test environments like anechoic or reverberation chambers, specifically given moderate dependence on DUT orientation.
4. With no conducting connection to the outside, monitoring under exposure is possible by optical fiber communication.
5. Custom software with GUI indicators facilitates monitoring.
6. We are ready to share the technical specification document.

Manuscript received July 13, 2020; revised August 27, 2020 and September 29, 2020; accepted September 29, 2020. Date of publication November 4, 2020; date of current version February 23, 2021. This work was supported by Bundeswehr Research Institute for Protective Technologies and NBC-Protection (WIS, Munster). *(Corresponding author: Thorsten R. Pusch.)*

The authors are with the Business Unit of Electromagnetic Effects and Threats, Fraunhofer Institute for Technological Trend Analysis, 53879 Euskirchen, Germany (e-mail: thorsten.pusch@int.fraunhofer.de; michael.suhrke@int.fraunhofer.de; benjamin.joerres@int.fraunhofer.de).

Digital Object Identifier 10.1109/LEMCPA.2020.3035893

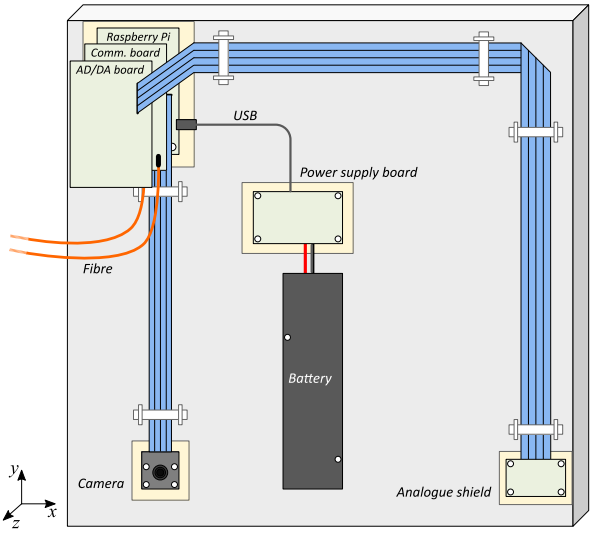

Fig. 1. Schematic overview of the test reference setup, showing the Raspberry Pi SBC as core component with peripherals connected via ribbon cabling. A battery-based power supply enables autarkic operation.

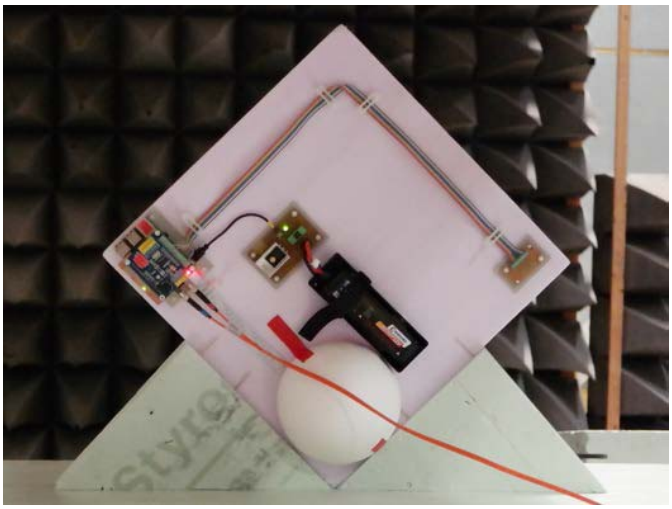

Fig. 2. The setup in the TEM waveguide, rotated by $-45°$ around the z-axis (see Fig. 1) for directivity measurements. A Styrofoam dome illuminated by the camera status led form the inside prevents ambient light from affecting video analysis. An optical fiber connects the setup to the control PC.

investigation of the dependency of error thresholds on DUT orientations for the present publication.

Keeping the direction dependency of coupling patterns in mind as a quantity playing into the comparison of plane wave test facilities like anechoic chambers with RC, we first of all show here our immunity profile data for two field orientations achieved by rotating the test setup by 90 degrees around its central axis. This is complemented by additional data roughly doubling the range of explored frequencies ending now at 8 GHz [7]. With these results established as a starting point, we do add here new results for another five DUT orientations at specific frequencies in order to extend the analysis of direction effects, while touching on a model regarding their potential frequency dependency proposed in [8].

II. The Reference Test Setup

A. Hardware Components

Our setup proposition mimicking everyday IT hardware is based on a single board computer (SBC) of the Raspberry Pi line of systems, combining long availability with affordability. Fixed at one corner of a square board of Styrofoam measuring 40 cm in edge length, it carries a communication board for serial communication as well as an AD/DA board, both affixed to the GPIO extension pins. A camera module complements the system by a digital sensor, while a voltage divider board connected to the AD/DA board which is applying and digitizing analogue voltages provides data for observing analogue effects. A schematic of the setup can be seen in Fig. 1, including the battery used for autarkic operation with its DC conversion PCB. The fixtures on ribbon cabling are meant to further reduce setup variance, as can be seen in the photograph in Fig. 2.

B. Long-Term Stability

With the intended use as a reference setup, we had to address the effect of electronics repeatedly exposed to high intensity signals physically deteriorating over time. Exchanging core components in the foreseeable future being unavoidable, the previous study had us investigate series variations across specimen of the Raspberry Pi 3 (V 1.2) SBC. A variation seldom exceeding 30% of the error threshold values would seem not to particularly discourage replacing worn out hardware. Spares should be available until 2026, by virtue of the longevity statement of the Pi Foundation.

TABLE I
Error Classification Scheme

Class	Description	Plot symbol
1	Analogue values out of tolerance	X
2	Video pixel values out of tolerance	O
3	Loss of serial link under exposure	□
4	Loss of serial link requiring restart	Δ

C. Error Classification and Monitoring Scheme

While a wide range of errors could previously be shown to occur, we have been narrowing them down to four classes [4]. If the digitized analogue voltages exceed a specified tolerance, an analogue error is diagnosed. Likewise, if a certain percentage of camera pixels deviates by more than a tolerance set to accommodate video noise from an averaged reference picture recorded on startup, a video error is noted. Finally, the serial connection could break down only under exposure or until restart, marking communication errors of class 3 and 4. Table I shows all error classes for reference.

Using an optical connection between the DUT and a monitoring PC located in the control room of the test facility, system states are continuously communicated to a control software with a graphical user interface, allowing for an easy overview of error states, including logging options.

D. Scheme for Immunity Testing

In our test facility at Fraunhofer INT, we used a tunable narrowband source system to inject rectangular pulses of typically

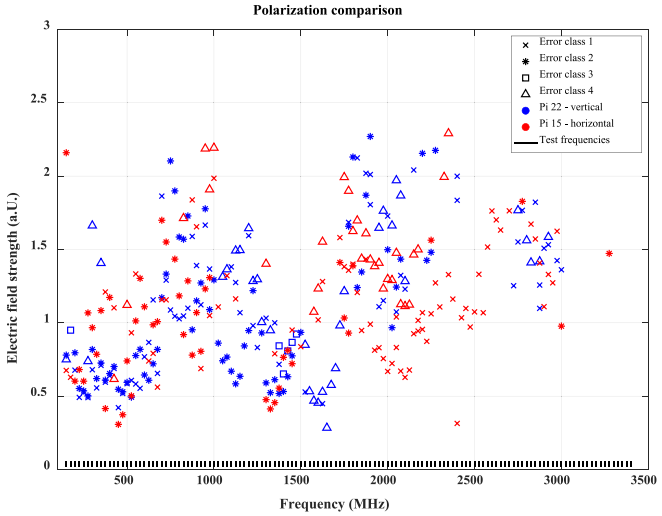

Fig. 3. Error thresholds for two different field polarizations, the setup being turned about 90 degrees.

1 µs in length, 1 kHz repetition rate and carrier frequencies in the range of 150 MHz up to 3.4 GHz into an open TEM waveguide where the DUT had been propped up on Styrofoam supports in various orientations, the electronics facing the incoming waves as seen in Fig. 2. Starting at a minimum value, we drove a power ramp of 20 s length upon which any error occurring was noted and assigned to a field strength value based on calibration data. Thus, characteristic immunity profiles were recorded, the frequency resolution depending on the use case.

III. Parameter Studies

In order to further investigate the setup's properties beyond our previous basic characterization [4] which validated high repeatability in measuring error threshold values, we varied the measurement conditions in a few parameter studies which will be detailed in the following. All failure thresholds are given as normalized electrical field strength values derived from waveguide calibration data gained with a field probe.

A. Vertical Versus Horizontal Polarization

When it comes to immunity measurements, the angle of incidence under which a DUT is illuminated will be relevant. Detailed immunity data with 25 MHz frequency resolution gained in the previous study [4] was complemented with the failure thresholds garnered on the setup rotated by its primary axis by 90 degrees [7]. Effectively, the incoming waves were now polarized horizontally, allowing us a first foray into the effect of directivity. As can be seen from the normalized failure threshold values plotted against test frequencies in Fig. 3, the global shape of the immunity profiles does not vary by much. Both profile envelopes share a global minimum at roughly 0.5 GHz as well as its third harmonic, which is aligning well with a coupling hypothesis of half a signal wavelength matching 30 cm long stretches of ribbon cabling.

Delving more into detail, some clustering of error symbols differs on a case by case basis., e.g., errors of class 4 clustering at 2 GHz for the horizontal polarization rather than 1.5 GHz as in the vertical case. Clearly, these effects will have to be taken into account when comparing to measurements in an RC. It should be noted that beyond 3 GHz, the source system is limited in dynamic range, thus preventing errors in the upper part of the plot from being detected.

B. Doubling the Covered Frequency Range

While we had gathered data up to 3.4 GHz in our previous study [4], we extended the test frequencies covered by our immunity measurements by a second range from 4 GHz up to 8 GHz by making use of a different source system. In addition, we repeated these measurements with the second polarization described earlier to be able to compare data. Within the dynamic range covered, similar errors could be induced at these higher frequencies, as shown in Fig. 4.

The previously seen trend of slightly rising values continues up to 5.5 GHz, from where on the immunity values dip twice until missing completely from 7.2 GHz onwards. Being able to trigger the known error patterns at higher frequencies and thus covering more of the frequency range typically referenced for potential IEMI attempts enhances the usability of the setup when it comes to standard development.

C. Probing the Effect of Further DUT Orientations

The measured immunity thresholds in a plane wave test environment will most probably miss the actual extremum by some extent, depending on the number of DUT orientations investigated. This gap could widen when going to higher frequencies at which the DUT can be considered "electrically large". Formally, this condition is met if $ka > 1$, k being the wave number $2\pi/\lambda$ and a the radius of the smallest sphere fully enclosing the DUT [8]. Its coupling characteristics can be described by an antenna pattern which resembles a dipole in the "electrically small" regime and increasingly fragments into various lobes at higher frequencies. Considering our setup with a maximum dimension of 40 cm, the above $ka = 1$ criterion is met at approx. 170 MHz. Due to the components being openly spread out on a Styrofoam board, the structure sizes relevant for coupling might scale down to a few cm, leading to a threshold value of roughly 925 MHz between the two regimes if considering the SBC dimensions of roughly 9 cm x 6 cm.

In order to further investigate such effects, we performed measurements at an additional five DUT orientations, now totaling in seven different rotation angles when including the previously shown data. We chose five triplets of test frequencies starting at 150 MHz and roughly doubling over each subsequent step. After measuring thresholds at the first three frequency clusters over all orientations, the central component was swapped in order to avoid potential bias by DUT deterioration. The results are shown in Fig. 5, the legend indicating the angle of rotation with respect to the coordinate axes drawn in Fig. 1.

As can be seen in the plot, some clustering of error thresholds is visible. Depending on the error category, values are spread out to some extent, clearly showing some directivity effects when comparing with the repetition accuracy of our measurements shown in [4]. Specifically at the two lowest frequency triplets, error class 1 thresholds lie very close together, while error class 2 values scatter a bit more.

It should be noted that while some errors would seem to show at less orientations when going to higher frequencies, this can be in part explained by the general trend of error

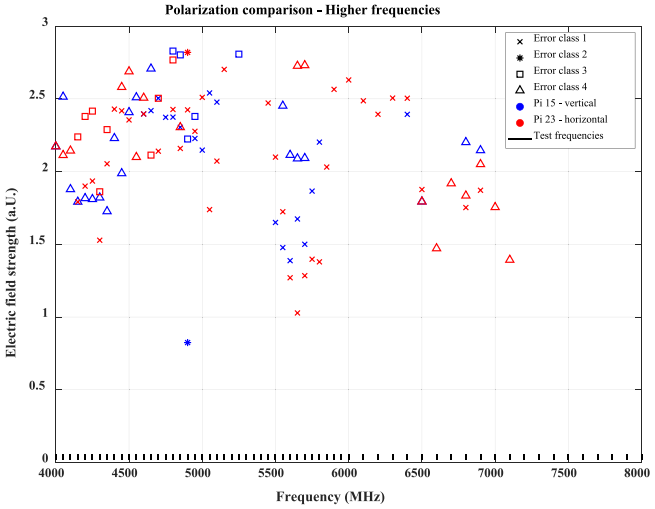

Fig. 4. Measurements over an extended frequency range to probe device immunity above 4 GHz.

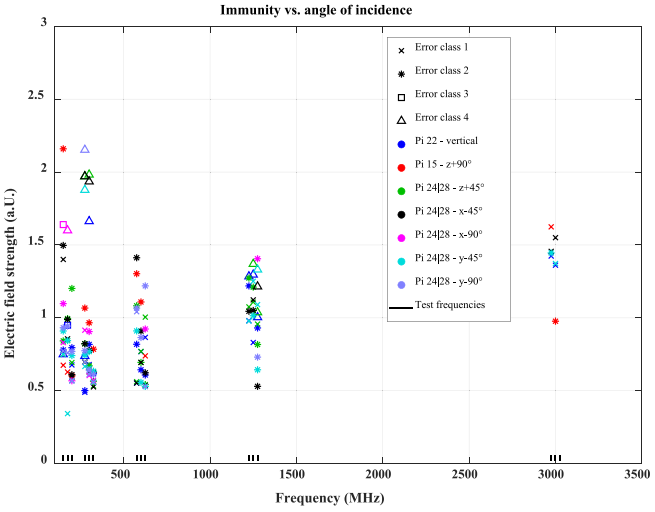

Fig. 5. Probing directivity by rotating the DUT around its axes. The respective excerpt of the results shown in Fig. 3 is included, keeping the symbol colors.

thresholds being on the rise which will push them out of the dynamic range of our source system.

In general, the error threshold values would seem not to particularly increase in spread going to higher frequencies, thus showing no clear evidence of an effect stemming from the aforementioned regimes of different electrical sizes. This could of course stem from the fact that the actual triggering of errors in the DUT not only depends on just coupling efficiency alone, but on the extent of interference with active signal processes in the system. In general, the moderate spread should bode well for comparison with measurement data collected in a reverberation chamber which inherently features very low dependency on DUT orientation.

IV. Conclusion

The basic premise of a reference test setup having been established, the investigations reported here were meant to further characterize the device behavior under different parameter combinations. Being able to extend frequency studies well beyond 4 GHz and thus covering a major part of the frequency range considered relevant for IEMI further validates the setup's versatility.

Regarding the influence of the angle of incidence of the plane waves on the DUT's failure thresholds, some differences can already be seen in just a binary comparison done in high frequency resolution over the whole available range. Aligning to some extent with respective norm prescriptions, the results at five additional DUT orientations could further elucidate a moderate dependency, albeit without aligning with an assumption of the value spread rising with frequency.

For the future, measurements in different test environments are planned, a first comparison with the RC results at one of our partner's facilities has already been performed [9]. Round-robin tests are intended to be carried out across participating laboratories. More specifically, interested parties intending to perform their own measurements are invited to have a look at our technical specifications document to be able to replicate the setup.

Analyzing present and future data collected with our reference test setup, we expect to be able to pinpoint more characteristics of the various test environments available, including a direct comparison of similar facilities.

Acknowledgment

The authors would like to thank their colleagues from the Bundeswehr Research Institute for Protective Technologies and NBC-Protection (WIS Munster, Germany) and from the Swedish Defence Research Agency FOI for the very constructive and fruitful collaboration.

References

[1] *Electromagnetic Compatibility (EMC)—Part 4-36: Testing and Measurement Techniques—IEMI Immunity Test Methods for Equipment and Systems*, IEC Standard 61000-4-36, 2014.

[2] *Electromagnetic Compatibility (EMC)—Part 5-9: Installation and Mitigation Guidelines—System-Level Susceptibility Assessments for HEMP and HPEM*, IEC/TS Standard 61000-5-9, 2009

[3] *Electromagnetic Environmental Effects Tests and Verification*, document AECTP-500 Edition E Version 1:2016, NATO, Brussels, Belgium, 2016.

[4] T. Pusch *et al.*, "A reference test setup to support research and development of HPEM testing schemes," in *Proc. Int. Symp. Electromagn. Compat. (EMC EUROPE)*, Barcelona, Spain, 2019, pp. 686–690, doi: 10.1109/EMCEurope.2019.8872105.

[5] F. Pythoud and E. Tas, "Design of a reference device for radiated immunity inter-laboratory comparison," in *Proc. Int. Symp. Electromagn. Compat. (EMC EUROPE)*, 2017, pp. 1–4, doi: 10.1109/EMCEurope.2017.8094672.

[6] S. Scheck, C. Paulwitz, and S. Weber, "Vergleichsuntersuchungen zwischen EMV-Laboratorien im Bereich der Störfestigkeitsprüfungen," in *Proc. EMV Int. Fachmesse und Kongress für Elektromagnetische Verträglichkeit*, Düsseldorf, Germany, 2018, pp. 118–125. [Online]. Available: https://doi.org/10.15488/4335

[7] T. Pusch, M. Suhrke, and B. Jörres, "Charakterisierung eines Referenztestaufbaus für die HPEM-Normenentwicklung," in *Proc. EMV Int. Fachmesse und Kongress für Elektromagnetische Verträglichkeit*, Köln, Germany, 2020, pp. 89–96. [Online]. Available: https://doi.org/10.15488/10014

[8] P. Wilson, "Emission and immunity testing: Test object electrical size and its implication," in *Proc. Int. Symp. Electromagn. Compat.*, vol. 2. Silicon Valley, CA, USA, 2004, pp. 349–352, doi: 10.1109/ISEMC.2004..

[9] T. Hurtig, M. Elfsberg, N. Wellander, T. Pusch, M. Schaarschmidt, and M. Suhrke, "A reference test setup and comparison between different HPEM testing schemes," in *Proc. Int. Symp. Electromagn. Compat. (EMC EUROPE)*, Rome, Italy, 2020, pp. 1–5, doi: 10.1109/EMCEUROPE48519.2020.9245826.